A Change in the Apparent *m* Value Reveals a Populated Intermediate under Equilibrium Conditions in *Escherichia coli* Ribonuclease HI[†]

Giulietta Spudich and Susan Marqusee*

Department of Molecular and Cell Biology, University of California, 229 Stanley Hall, Berkeley, California 94720

Received February 29, 2000; Revised Manuscript Received June 5, 2000

ABSTRACT: Experimental studies of protein stability often rely on the determination of an "*m* value", which describes the denaturant dependence of the free energy change between two states ($\Delta G = \Delta G_{H_2O} - m$[denaturant]). Changes in the *m* value accompanying site specific mutations are usually attributed to structural alterations in the native or unfolded ensemble. Here, we provide an example of significant reduction in the *m* value resulting from a subtle deviation in two-state behavior not detected by traditional methods. The protein that is studied is a variant of *Escherchia coli* RNase H* in which three residues predicted to be involved in a partially buried salt bridge network were mutated to alanine (R46A, D102A, and D148A). Equilibrium denaturant profiles monitored by both fluorescence and circular dichroism appeared to be cooperative, and a two-state analysis yielded a ΔG_{UN} of approximately −3 kcal/mol with an *m* value of 1.4 kcal mol^{-1} M^{-1} (vs 2.3 for RNase H*). Analysis of kinetic refolding experiments suggests that the system is actually three-state at equilibrium with an appreciable concentration of an intermediate state under low denaturant concentrations. The stability of the native state determined from a fit of these kinetic data is −6.7 kcal/mol, suggesting that the stability determined by traditional two-state equilibrium analysis is a gross underestimate. The only hint to this loss of two-state behavior was a decrease in the apparent *m* value, and the presence of the equilibrium intermediate was only identified by a kinetic analysis. Our work serves as a cautionary note; the possibility of a three-state system should be closely addressed before interpreting a change in the *m* value as a change in the native or unfolded state.

The three-dimensional structure and stability of a protein are determined by a cooperative network of tertiary interactions. The relative importance of each of these interactions is often evaluated using site-specific mutagenesis in a so-called protein engineering approach. This approach, however, can yield deceptive results. Point mutations can cause unpredicted changes, altering the basic properties of the protein. Such changes can be dramatic and obvious (such as causing the protein to unfold under previously native conditions), or they can be masked and difficult to detect.

In addition to changes in the overall stability of the protein, point mutations often change a protein's apparent "*m* value" [a parameter describing the dependence of stability on denaturant (*1*)]. The basis for these changes is controversial. The folding stability of a protein, ΔG_{UN} [the change in free energy between the unfolded (U) and the folded state (N)], is thought to be linearly dependent on chemical denaturants such as urea or GdmCl (*2*); $\Delta G = \Delta G_{H_2O} - m$[denaturant], where the *m* value is thought to correlate with the difference between accessible hydrophobic surface areas in the unfolded and folded states (*3*−*5*). Changes in *m* value, therefore, are usually attributed to changes in the conformations of either the folded or unfolded ensemble. Since most single-site mutations do not dramatically affect the structure of a protein, large changes in the *m* value (particularly decreases) have been ascribed to changes in the unfolded ensemble (*4*). Implicit in this rational is the assumption that the system is two-state, and only the native and unfolded states are populated (U ↔ N). Population of a third state, or intermediate, could also result in a decrease in the apparent *m* value (U ↔ I ↔ N) (*6*, *7*).

Here, we demonstrate a change in the apparent *m* value arising from a subtle deviation from two-state behavior due to the population of an intermediate not detected by traditional means. The potential for a multistate system to have an apparently cooperative denaturant transition has been noted in the literature (*7*, *8*). We observe an experimental example of this phenomenon, and lend a cautionary note to investigators, showing that it can be difficult to rule out such deviations. Such a subtle and undetected deviation from two-state behavior could explain discrepancies in the literature between the free energy derived from denaturant melts and that derived by other means, such as hydrogen−deuterium exchange (*9*).

In this work, our initial goals were to analyze the energetics of a buried salt bridge network composed of one Arg residue and two Asp residues in *Escherichia coli* RNase H*[1] (Figure 1) (*10*, *11*). To measure the free energy of interaction between these residues, we constructed a series of mutant proteins to be used in a thermodynamic analysis, based on

[†] This work was supported by a grant from the NIH (GM50945).

* To whom correspondence should be addressed. Telephone: (510) 642-7678. Fax: (510) 643-9290. E-mail: marqusee@uclink4.berkeley.edu.

[1] Abbreviations: CD, circular dichroism; GdmCl, guanidinium chloride; RNase H, *E. coli* ribonuclease HI; RNase H*, fully active variant of RNase H in which three free cysteines are replaced with alanine; R46A/D102A/D148A, triple-mutant protein of RNase H* in which all three indicated residues are replaced with alanine.

10.1021/bi000466u CCC: $19.00
Published on Web 08/25/2000

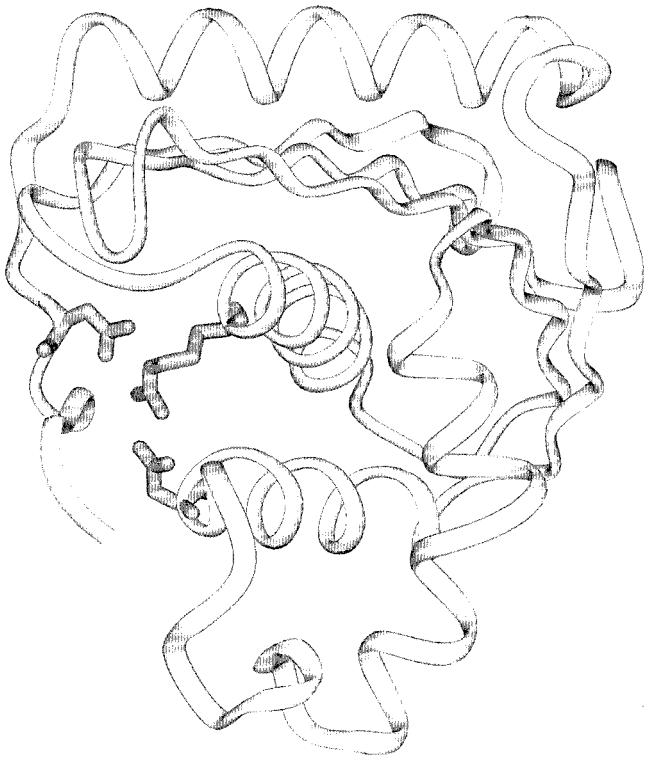

FIGURE 1: Crystal structure of *E. coli* RNase HI containing a partially buried salt bridge network (*11*). The three side chains that are involved are shown (R46, D102, and D148). This putative network of interactions involves atoms less than 3 Å apart.

the free energy of unfolding determined for each of the variants obtained by standard chemical denaturation studies. This method, pioneered by Fersht and co-workers (*12*−*15*), is the most common method of assessing the interaction energy between residues. The equilibrium denaturant profiles obtained here exhibited apparent two-state behavior in all respects, with the singular concern of lowered *m* values. A three-state kinetic analysis (U ↔ I ↔ N) of the refolding of one of these low-apparent *m* value mutants revealed that the transient intermediate (I) has a stability and *m* value such that it is significantly populated during the equilibrium studies. While the wild-type protein also folds via a kinetic intermediate, it only significantly populates the native and unfolded states under the same conditions.

The only clue to the deviation from two-state behavior of the equilibrium system of the variant was the apparent low *m* value, and a kinetic approach was necessary to determine the true equilibrium stabilities and populations of the native, unfolded, and intermediate states. Without an *m* value of the wild-type protein for comparison, traditional equilibrium denaturation melts would have missed this intermediate and have been extremely inaccurate in determining the stability of the protein.

MATERIALS AND METHODS

Construction of the Triple Mutant. Site-directed mutagenesis of R46 or D148 to alanine was performed on a cysteine-free variant of *E. coli* RNase H (RNase H*), encoded in the plasmid pSM101 (*16*) using the standard Kunkel method (*17*). The resulting plasmids containing single mutations, together with pTA202 (encoding D102A), were digested and religated to yield pGS300, which encodes all three mutations. This plasmid encodes the RNase H* protein with mutations R46A, D102A, and D148A and is termed R46A/D102A/D148A, or simply the triple mutant.

Protein Expression and Purification. pGS300 was transformed into *E. coli* BL21 pLysS (Novagen) cells. Cells were grown at 37 °C in Luria-Bertani (LB) medium with 100 mg/mL ampicillin. Induction of R46A/D102A/D148A was obtained by addition of 1 mM IPTG to cells in midlog phase ($OD_{600} \sim 0.6$). Cells were grown 3 h after induction, and were harvested by centrifugation. The protein was found in inclusion bodies, and purification was carried out on cell pellets using the protocol previously described for other RNase H variants (*18*). The protein obtained from this preparation was purified by reversed-phase HPLC, and the purity and molecular weights were verified by mass spectroscopy (data not shown). The protein was then lyophilized and stored at 4 °C.

Equilibrium CD and Fluorescence Experiments. Circular dichroism (CD) measurements were carried out on an Aviv 62DS spectrometer with a Peltier temperature-controlled cell holder. All CD experiments were carried out in 20 mM KH_2PO_4 and 50 mM KCl at pH 5.5. To measure the CD signal as a function of temperature, the sample (50 μg/mL protein in 0.5 M GdnHCl) was allowed to equilibrate for 4 min at each temperature (data were collected at 222 nm every 3 °C with a path length of 1 cm). Under these conditions, denaturation is reversible, as seen by comparison of spectra at 4 °C before and after the thermal melt.

For chemical denaturation studies, samples at different urea concentrations were made up individually (50 μg/mL protein and the indicated urea concentration) and were allowed to equilibrate at room temperature overnight. These samples were probed by both CD and fluorescence. The CD signal was measured at 222 nm, and data were averaged over a 3 min window.

These same samples were also evaluated by intrinsic fluorescence in a Perkin-Elmer LS50B luminescence spectrophotometer, using an excitation wavelength of 295 nm. Emission spectra were collected from 300 to 400 nm. The signal at 374 nm (the maximum of the unfolded signal) was divided by the signal at 324 nm (the maximum of the folded signal) for each sample, and the resulting signal was plotted against urea concentration.

Two-State Analysis of Equilibrium Experiments. Temperature melts were fit to a two-state model, using the Gibbs−Helmholtz relationship (*19*). Urea denaturation profiles were fit using a two-state assumption, and a linear extrapolation (*20*):

$$\Delta G_{UN} = \Delta G_{H_2O} - m[\text{denaturant}] \qquad (1)$$

CD Spectra. Spectra were recorded on the denaturant melt sample containing 0 M urea. The signal was measured every nanometer between 290 and 190 nm, and the average signal over 1 s was collected for each wavelength. This was repeated three times, and the average of these spectra was obtained.

Kinetic Folding Experiments. Refolding was initiated by a 1:11 dilution of an unfolded stock [2.2 mg/mL R46A/D102A/D148A, 4.5 M urea, 20 mM KH_2PO_4, and 50 mM KCl (pH 5.5)] into refolding buffer (20 mM KH_2PO_4, 50 mM KCl, and the appropriate concentration of urea) in an

Aviv 202SF circular dichroism spectrometer (using a delta mixer and a path length of 1 mm). Unfolding experiments were carried out in a similar fashion, using a folded stock solution [2.2 mg/mL protein, 0 M urea, 20 mM KH_2PO_4, and 50 mM KCl (pH 5.5)].

Analysis of Kinetic Data. SFCD data were fit to single exponentials, using Sigma Plot for Windows (version 4, SPSS Inc.):

$$\text{signal} = A \exp^{-k_{obs}t} + C \quad (2)$$

where C is the final amplitude, A is the amplitude of the observable phase, t is time, and k_{obs} is the observed rate constant. The amplitude of the burst phase, A_{bp} (in the refolding experiments, completed within the ~15 ms dead time of the instrument), was calculated via

$$A_{bp} = (C + A) - \text{the unfolded signal} \quad (3)$$

Since only amplitudes can be determined for the burst phase, this amplitude may represent one or more phases. In the simplest model, the burst phase amplitudes describe a two-state system (U ↔ I); thus, they were fit using a linear extrapolation. Observed rates were then fit to a three-state on-pathway model:

$$\text{U} \overset{K_{UI}}{\longleftrightarrow} \text{I} \underset{k_{NI}}{\overset{k_{IN}}{\rightleftharpoons}} \text{N} \quad (4)$$

using the following equation:

$$\ln k_{obs} = \ln[[K_{UI}/(1 + K_{UI})]k_{IN(DEN)} + k_{NI(DEN)}] \quad (5)$$

where K_{UI} and m_{UI} describe the equilibrium constant and the m value between U and I obtained from the burst phase amplitudes, respectively, and $k_{IN(DEN)}$ and $k_{NI(DEN)}$ (the folding and unfolding microscopic rate constants for the equilibrium between I and N, respectively) and m_{IN} and m_{NI} (the denaturant dependencies of these rate constants) are described as follows (where x is the urea concentration, R is the gas constant, and T is the temperature):

$$k_{IN(DEN)} = k_{IN(H_2O)} \exp(-m_{IN}x/RT) \quad (6)$$

$$k_{NI(DEN)} = k_{NI(H_2O)} \exp(-m_{NI}x/RT) \quad (7)$$

Calculation of ϕ Values. ϕ values were calculated using parameters obtained from the three-state on-pathway fit of the kinetic data. The ϕ value of the I state was calculated as follows:

$$\phi_I = [\Delta G_{UI(WT)} - \Delta G_{UI(MUT)}]/[\Delta G_{UN(WT)} - \Delta G_{UN(MUT)}] \quad (8)$$

The ϕ value for the folding transition state of the mutant was calculated using the following equation:

$$\phi^{\ddagger} = 1 - \{RT \ln[k_{IN}(\text{mut})/k_{IN}(\text{wt})]/[\Delta G_{UN(WT)} - \Delta G_{UN(MUT)}]\} \quad (9)$$

Modeling of the Equilibrium System from Kinetic Data. K_{UN} and m_{UN} were calculated from values obtained from the kinetic experiments using the following relationships: $m_{UN} = m_{UI} + m_{IN} - m_{NI}$, and $K_{UN} = K_{UI}k_{IN(H_2O)}/k_{NI(H_2O)}$. The fractions of I and N populated at equilibrium were calculated from the equilibrium constants, and the fraction of U populated was modeled as fraction U = 1 − (fraction I + fraction N).

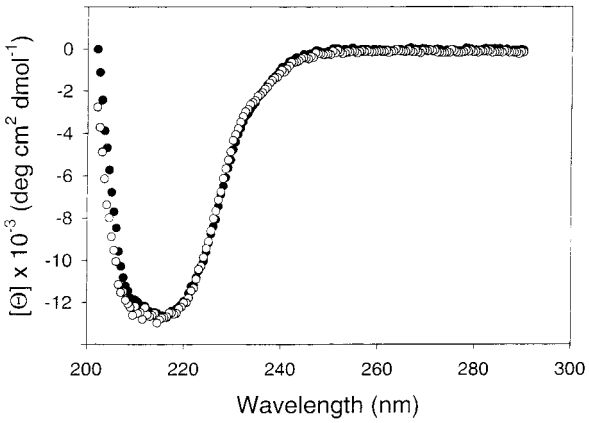

FIGURE 2: Circular dichroism spectrum of the triple mutant (R46A/D102A/D148A) (○) overlaying that of RNase H* (●). Spectra were collected at 25 °C and pH 5.5.

RESULTS

To investigate the role of the salt bridge network between R46, D102, and D148 in RNase H, we constructed a series of mutants in which one or more of these residues were converted to alanine. In this paper, we present the results for just one of these variants, the triple mutant (R46A/D102A/D148A), although several of the variants exhibited similar behavior. Low-resolution structural data suggest that the basic fold of the native state of the protein is preserved in the triple mutant. The far-UV CD spectra of the two are indistinguishable as seen in Figure 2. The triple mutant also retains RNase H activity, as assayed by monitoring the change in UV absorption of a poly(rA-dT) template at 260 nm (data not shown).

Equilibrium Studies. All of the equilibrium unfolding studies suggest that, like RNase H*, the triple mutant follows two-state behavior, populating either the native or unfolded state. Thermal denaturation studies monitored by far-UV CD were fully reversible in the presence of 0.5 M GdmCl and demonstrated a cooperative transition, albeit one broader than that of RNase H* (Figure 3). The data fit easily to a two-state model, yielding a T_m of 46 °C, much lower than the T_m of RNase H* (61 °C).

Urea-induced denaturation monitored by far-UV CD also resulted in a cooperative, apparently two-state curve (Figure 4). The free energy of folding ΔG_{UN} derived from this two-state fit (see Materials and Methods) is extremely low (−3.2 kcal/mol) compared with that from RNase H* (−10.0 kcal/mol), suggesting a ~7 kcal/mol decrease in the stability due to these mutations. This urea denaturation profile also appeared to be cooperative when monitored by intrinsic fluorescence. Fluorescence emission spectra taken at varying urea concentrations were not in violation of a two-state transition, as we could not clearly determine the absence of an isosbestic point (Figure 5). The standard two-state linear extrapolation fit of the fluorescence data resulted in a free energy of folding that was slightly (~0.7 kcal/mol) higher than that obtained by CD, but within the experimental error,

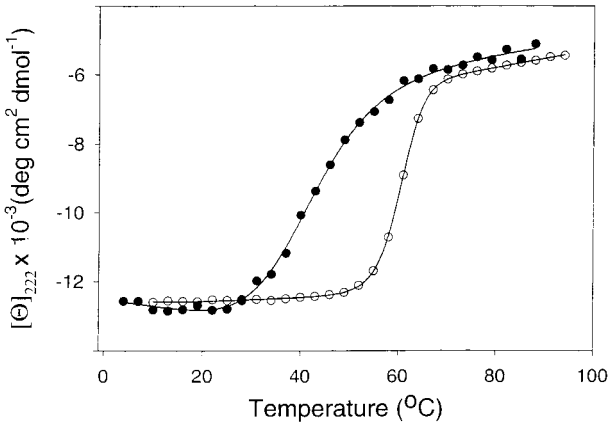

FIGURE 3: Thermal denaturations of *E. coli* RNase H* (○) and R46A/D102A/D148A (●) appear to be cooperative. Data were collected by monitoring the circular dichroism (CD) signal at 222 nm as a function of temperature. Lines correspond to two-state fits of each data set (see Materials and Methods). Melts were reversible [determined by comparison of spectra at 4 °C before and after denaturation (data not shown)].

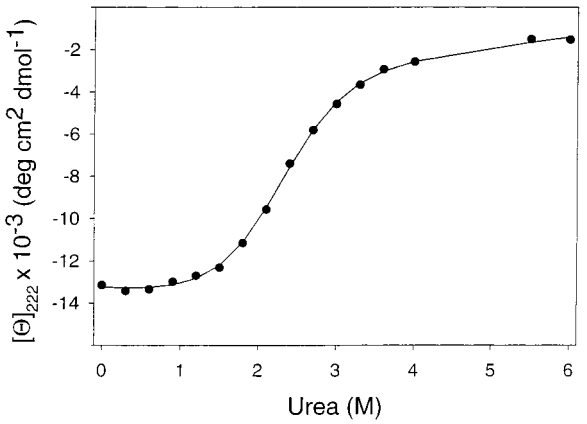

FIGURE 4: Urea-induced denaturation of R46A/D102A/D148A examined by CD which appears to be cooperative. Each point (●) corresponds to the average CD signal at 222 nm over a 2 min interval of an individual sample allowed to equilibrate overnight. The curve corresponds to a fit of the data to a two-state model, which yields a ΔG_{UN} of -3.2 kcal mol^{-1} (RNase H* $\Delta G_{UN} = -9.7$) and an m_{UN} of 1.4 kcal mol^{-1} M^{-1} (RNase H* $m_{UN} = 2.1$).

suggesting the coincident loss of tertiary structure and secondary structure (i.e., a two-state system).

Surprisingly, the *m* value associated with the urea-induced denaturation transition was very low (1.4 ± 0.1 kcal M^{-1} mol^{-1} as compared with 2.1 ± 0.1 kcal M^{-1} mol^{-1} for RNase H*). Changes in the *m* value have been interpreted to result from either perturbations in the structure of the native or unfolded state or a deviation from a simple two-state transition (U ↔ N).

Although the change in the *m* value appears to be significant, we were unable to infer any dramatic alterations in the structures of N or U. Both the activity and CD spectra indicate no major perturbations in the native state. It seems unlikely that there are significant perturbations in the unfolded ensemble since the three residues involved are distant in sequence space (residues 46, 102, and 148). Furthermore, the *m* value changes in the variants do not correlate with hydrocarbon deletion; for example, the *m* value corresponding to the triple mutant, R46A/D102A/D148A, is slightly greater than the *m* value obtained for a single

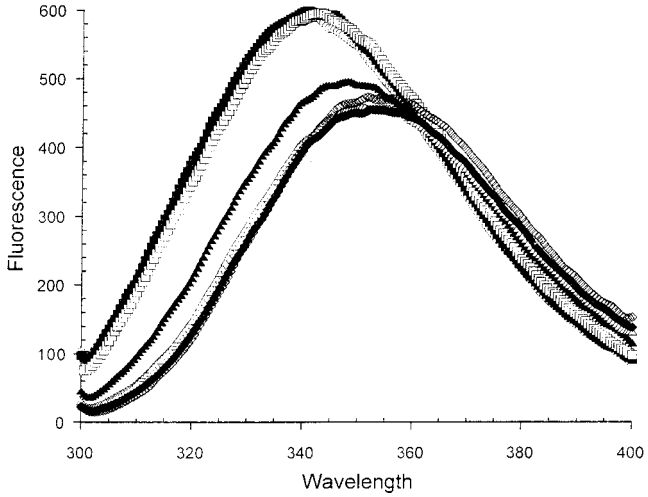

FIGURE 5: Intrinsic fluorescence spectra of R46A/D102A/D148A at various denaturant concentrations exhibiting an isosbestic point. Spectra were obtained using a Perkin-Elmer LS50B luminescence spectrophotometer at 10 °C for each sample in the denaturant melt (monitored by CD as seen in Figure 4). Samples were excited at 295 nm, and emission spectra were collected between 300 and 400 nm. Spectra are shown for samples at urea concentrations of 0.4, 0.9, 1.7, 2.5, 3.0, 3.5, and 4.4 M (○, ■, □, ▲, △, ◆, and ◇, respectively).

mutant, D148A (1.5 vs 1.3 kcal M^{-1} mol^{-1}, data not shown). Therefore, even though the equilibrium experiments resembled two-state behavior, the large drop in the observed *m* value led us to question the validity of the two-state approximation.

Kinetic Studies. The refolding and unfolding kinetics of the triple mutant were investigated by stopped-flow CD. Analysis of the apparent rates as a function of the final urea concentration resulted in the so-called "chevron plot" shown in Figure 6A. The apparent "V" shape of this curve hints at a two-state system; however, the presence of a burst phase in the refolding experiments (~80% of the native CD signal was regained within the ~15 ms dead time of the instrument) suggests the existence of three states with a transient burst phase intermediate (U ↔ I ↔ N). Refolding of RNase H* shows a similar burst-phase intermediate; in this case, however, the transient population of the intermediate results in an observed rollover in the chevron plot (*21*).

Since the observed rate is much (more than 300 times) slower than the burst-phase process, the amplitude of the burst phase represents a kinetically uncoupled pre-equilibrium between the intermediate and unfolded states (*22*). A plot of this burst-phase amplitude as a function of final denaturant concentration (Figure 6B) reveals a cooperative transition very similar to the burst-phase intermediate in RNase H*. The resulting free energy (ΔG_{UI}) and m_{UI} are all similar to those of RNase H* (Table 1). In combination with the results of the fit of the burst-phase amplitudes, the apparent rate constants, or chevron plot, were easily fit to a three-state on-pathway kinetic mechanism (U ↔ I ↔ N). While in RNase H* transient formation of this early kinetic intermediate produces an easily visible so-called "rollover effect" (*23*), the lack of this feature in the variant protein can be attributed to an extended rollover dominating the entire folding limb of the chevron plot. The individual rate constants and equilibrium constants obtained from this three-state analysis can be used to determine an overall free energy

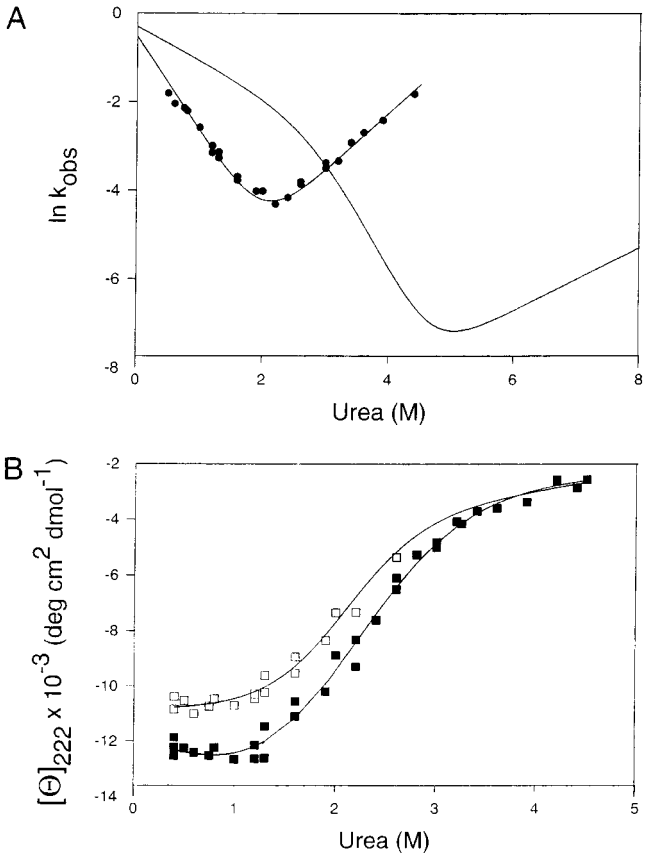

FIGURE 6: Relaxation kinetics of R46A/D102A/D148A as determined on an Aviv 202 stopped-flow circular dichroism spectrometer at 222 nm and 25 °C. Data from folding and unfolding reactions at varying concentrations of urea were fit to single exponentials, and a burst phase was seen in the folding kinetics, which we interpret as an early kinetic transient (*22*). (A) Observed rates (●) obtained from single-exponential fits of the folding and unfolding reactions are shown as a function of denaturant in the chevron plot. A three-state on-pathway fit of these rates is plotted as a line (parameters shown in Table 1). Note that the entire folding arm is influenced by the intermediate state; thus, the folding half of the chevron exists within the rollover. The fit corresponding to the RNase H* is shown for comparison (*22*). (B) Burst-phase amplitudes (□) obtained from the folding experiments were plotted as a function of urea concentration and fit using a two-state assumption (corresponding curve). The parameters obtained closely resemble those for the RNase H* intermediate state (see Table 1). A fit of the equilibrium denaturant melt (refer to Figure 4) corresponds to the final amplitudes from kinetic experiments (■ and the corresponding curve). A two-state fit of the final amplitudes yields the same parameters as the fit of the equilibrium melt.

change (and associated *m* value) for the equilibrium between U to N (Table 1). For the triple mutant, ΔG_{UN} obtained from the three-state kinetic analysis is −6.7 kcal/mol, a value much higher than that obtained from the two-state fit of the urea melt (−3.2 kcal/mol). There is no discrepancy in the ΔG_{UN} for RNase H* measured by these two methods.

DISCUSSION

We initially set out to analyze the energies of the interaction between three residues of a buried salt bridge network in *E. coli* RNase H. We began by using the traditional method of obtaining free energies of unfolding of a series of variants using equilibrium denaturant melts. During these experiments, we noted that although the equilibrium denaturation curves of these variants appeared

Table 1: Thermodynamic Parameters for *E. coli* RNase H* and R46A/D102A/D148A (the triple mutant)

	E. coli RNase H*[a]	R46A/ D102A/D148A[b]
apparent ΔG_{UN} (kcal mol^{-1}) (two-state fit)	−9.7 ± 0.4	−3.2 ± 0.3
ΔG_{UN} (kcal mol^{-1}) (three-state fit)	−9.9	−6.7
apparent m_{UN} (kcal mol^{-1} M^{-1}) (two-state fit)	2.1 ± 0.1	1.4 ± 0.1
m_{UN} (kcal mol^{-1} M^{-1}) (three-state fit)	2.1	3.2
ΔG_{UI} (kcal mol^{-1}) (three-state fit)	−3.6	−3.1 ± 0.04
m_{UI} (kcal mol^{-1} M^{-1}) (three-state fit)	1.2	1.5 ± 0.02
k_{IN} (H_2O) (s^{-1})	0.74	0.33 ± 0.04
m_{IN} (kcal mol^{-1} M^{-1})	0.454	0.94 ± 0.06
k_{NI} (H_2O) (s^{-1})	1.69×10^{-5}	$(7.95 \pm 1.6) \times 10^{-4}$
m_{NI} (kcal mol^{-1} M^{-1})	−0.422	−0.72 ± 0.4
ϕ_I	−	0.1
$\phi^{\ddagger}$	−	0.3

[a] The parameters for wt* were previously obtained (*22*). [b] Three-state parameters were obtained by an analysis of kinetic data. Apparent free energies and *m* values obtained by two-state treatment of equilibrium data are included for comparison.

to be two-state, the resulting *m* values were significantly lower than that of RNase H*. Hence, we decided to investigate one of these variants (R46A/D102A/D148A) more closely. Kinetic refolding studies on this triple mutant demonstrated the presence of a transient intermediate formed within the dead time of the instrument. The data were easily fit to a three-state, on-pathway model (U ↔ I ↔ N). This three-state fit yielded a free energy of folding (ΔG_{UN}) and an overall *m* value that were much higher than those of the two-state fit of the denaturant profile (which was thought to reflect only U and N). These differences can be reconciled by taking into account the small but significant population of the intermediate present in the transition zone under equilibrium conditions

The individual equilibrium and rate constants as well as the corresponding *m* values obtained from the fit of the kinetic data were used to model the populations of all three states (U, I, and N) at equilibrium. Surprisingly, this analysis revealed that for the triple mutant under low denaturant concentrations, all three states are populated at equilibrium (Figure 7A). Similar treatment of the RNase H* kinetic data predicts only two states (U and N) populated in the RNase H* protein at all denaturant concentrations under equilibrium conditions, as expected (Figure 7B). While the equilibrium data for both proteins can easily be fit to two-state denaturation curves, the ΔG_{UN} and overall *m* value obtained in this manner are erroneous in the case of the triple mutant.

The results from the three-state fit of the kinetic data model the observed equilibrium behavior of the protein (Figure 8). The broad transition melt of the triple mutant is therefore not a result of a low *m* value, but rather a reflection of a small but significant population of a third state (I) in the transition region of the curve.

The three-state fit of the kinetic data reveals that while the mutation R46A/D102A/D148A severely destabilizes the native state (U ↔ N) ($\Delta\Delta G_{UN} \sim 3$ kcal/mol), it does not affect the stability of the kinetic intermediate (U ↔ I) ($\Delta\Delta G_{UI} \sim 0$ kcal/mol). The specific destabilization of the native state

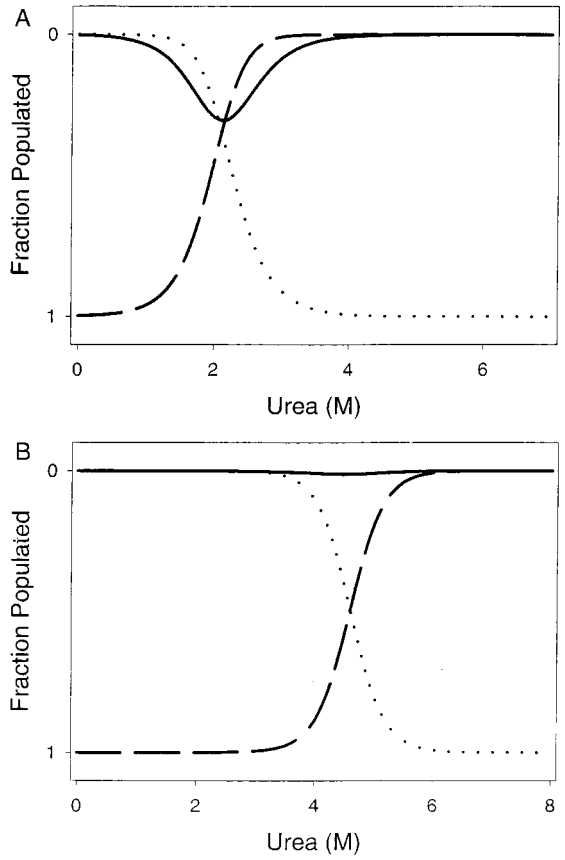

FIGURE 7: Observed microscopic rate constants obtained from kinetic experiments were used to model the system at equilibrium (as described in Materials and Methods). (A) The intermediate (I) state is populated under low denaturant concentrations in the triple mutant. The equilibrium system is three-state due to the small stability difference between the I and N (native) states. (B) The kinetic intermediate is not populated in RNase H* under these conditions, and the system is two-state at equilibrium.

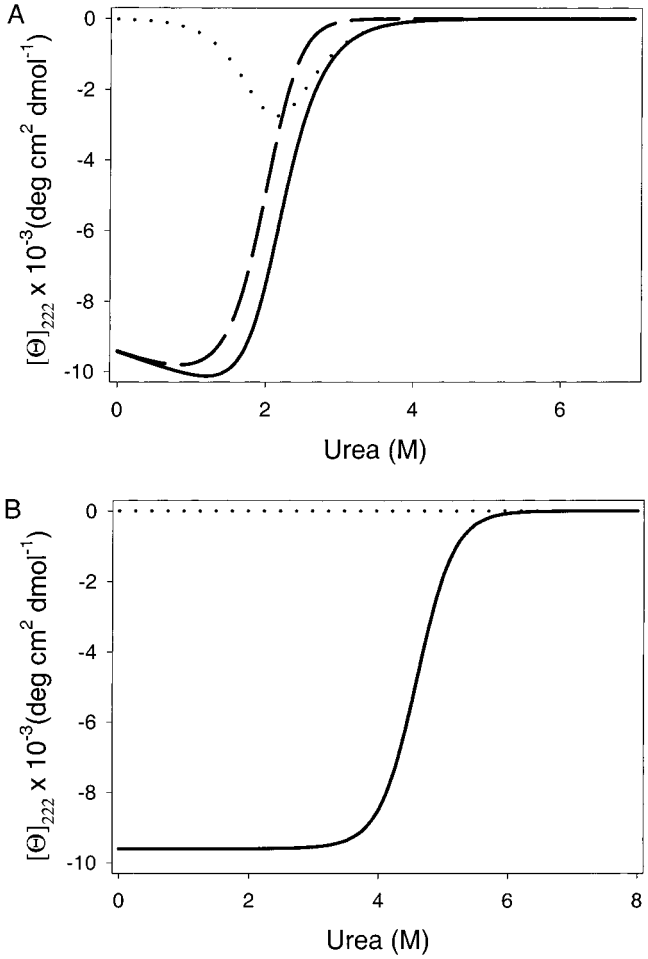

FIGURE 8: Kinetic data were used to simulate the contributions of I (dotted curve) and N (dashed curve) to the CD signal observed at equilibrium (solid curve). Individual contributions were obtained by multiplying the populated fraction of each state by its intrinsic CD signal. The total predicted signal overlays the actual equilibrium experiment. (A) The I state makes a substantial contribution to the CD signal at low denaturant concentrations in the triple mutant. The CD signal observed reflects both the I and N states, and reflects an apparent *m* value that is much lower than that of the N state. (B) The I state is not populated at any denaturant concentration measured in the RNase H* protein, and the signal due to the N state exactly overlays the total observed CD signal.

results in a relatively small difference in stability between N and I. It is this small difference in ΔG_{IN} which gives rise to an equilibrium population of I in the transition zone not seen in RNase H* under the same conditions. The selective effect on the native state is consistent with the idea that long-range electrostatic interactions are much more important to the native state than to the heavily solvated kinetic intermediate (*24*).

Our work highlights the fact that the *m* value is an important parameter in the determination of protein stability. The change in the *m* value of the variant protein was the only indicator of deviation from two-state behavior. Using the faulty free energy obtained with a two-state model of this three-state system would have caused us to calculate a grossly incorrect free energy of interaction in the salt bridge network. The two-state analysis of the denaturant melt yields a free energy of folding that is only half of the actual value (−3.2 vs −6.7 kcal/mol). This is not a subtle difference, and it is clear to us that we cannot trust the values derived by two-state fits of the denaturant melts. In our system, we had to turn to kinetic studies to elucidate the free energy of folding for these mutant proteins.

Our work provides an example of a decrease in the *m* value that is not a consequence of a change in solvent-accessible surface area of either the native or unfolded ensemble. The nature of the *m* value and a change in this parameter have been a topic of much discussion. This controversy is most apparent in the debate over mutants of staphylococcal nuclease (SN), where evidence suggests that changes in the *m* value in mutants of this protein can be ascribed to an increase or decrease in the stability of the denatured ensemble (*4*, *25*−*27*). Our work does not resolve the questions over SN; however, we show how difficult it can be to rule out the presence of an intermediate state in the equilibrium analysis of a system.

Recently, Wrabl and Shortle examined several SN variants with low *m* values using hydrogen exchange (*9*). They identified regions of "super protection" (protection factors correspond to a free energy greater than that expected for the global unfolding in an *m* value mutant) and suggest that these unusual protection factors are a result of structure in the unfolded ensemble hindering hydrogen exchange. It should be noted, however, that our three-state system would also be expected to demonstrate super protection (level of protection greater than that expected on the basis of the

equilibrium studies). These protection factors would correspond to the true global stability of the protein (ΔG_{UN}) and would not necessarily reflect structure in the unfolded state.

Our work provides a clear example of a lowered *m* value due to the presence of an intermediate state that escaped detection when probed by traditional means. Clearly, it can be difficult to rule out the population of an intermediate in a system, and care should be given when interpreting an *m* value obtained by a denaturant melt as an intrinsic property of the native or unfolded protein.

In summation, a change in the apparent *m* value of a denaturant melt is usually attributed to a change in the structure in N or U if the system is shown to be two-state through traditional probes at equilibrium. In our system, traditional methods for determining two-state behavior fail. These methods include the detection of cooperative melting curves and apparent coincidence of probes (for example, CD and fluorescence). The latter could be expected in a three-state system if, for example, the I state had a fluorescence signal similar to that of the N state. In our system, the only warning signal that the system had been converted from two to three states at equilibrium was the low *m* value. Our studies show that a change in the *m* value can signify the presence of an intermediate state in a denaturant melt which appears in other ways to be two-state. Nontraditional methods, such as kinetic studies, may be required to resolve the stabilities of the three states that exist at equilibrium.

ACKNOWLEDGMENT

We thank David King for mass spectrometry and Jack Kirsch for the use of his fluorimeter. We thank J. Martin Scholtz, Eric Goedken, and Eric Nicholson for critical reading of the manuscript and members of the Marqusee laboratory for support and advice.

REFERENCES

1. Greene, R. F., Jr., and Pace, C. N. (1974) *J. Biol. Chem. 249*, 5388−5393.
2. Pace, C. N. (1986) *Methods Enzymol. 131*, 266−280.
3. Tanford, C. (1970) *Adv. Protein Chem. 24*, 1−95.
4. Shortle, D. (1995) *Adv. Protein Chem. 46*, 217−247.
5. Myers, J. K., Pace, C. N., and Scholtz, J. M. (1995) *Protein Sci. 4*, 2138−2148.
6. Creighton, T. E., and Shortle, D. (1994) *J. Mol. Biol. 242*, 670−682.
7. Soulages, J. L. (1998) *Biophys. J. 75*, 484−492.
8. Eftink, M. R., and Ionescu, R. (1997) *Biophys. Chem. 64*, 175−197.
9. Wrabl, J., and Shortle, D. (1999) *Nat. Struct. Biol. 6*, 876−883.
10. Katayanagi, K., Miyagawa, M., Matsushima, M., Ishikawa, M., Kanaya, S., Nakamura, H., Ikehara, M., Matsuzaki, T., and Morikawa, K. (1992) *J. Mol. Biol. 223*, 1029−1052.
11. Yang, W., Hendrickson, W. A., Crouch, R. J., and Satow, Y. (1990) *Science 249*, 1398−1405.
12. Carter, P. J., Winter, G., Wilkinson, A. J., and Fersht, A. R. (1984) *Cell 38*, 835−840.
13. Horovitz, A. (1987) *J. Mol. Biol. 196*, 733−735.
14. Ackers, G. K., and Smith, F. R. (1985) *Annu. Rev. Biochem. 54*, 597−629.
15. Horovitz, A., and Fersht, A. R. (1990) *J. Mol. Biol. 214*, 613−617.
16. Dabora, J. M., and Marqusee, S. (1994) *Protein Sci. 3*, 1401−1408.
17. Kunkel, T. A. (1985) *Proc. Natl. Acad. Sci. U.S.A. 82*, 488−492.
18. Goedken, E. R., Raschke, T. M., and Marqusee, S. (1997) *Biochemistry 36*, 7256−7263.
19. Becktel, W. J., and Schellman, J. A. (1987) *Biopolymers 26*, 1859−1877.
20. Santoro, M. M., and Bolen, D. W. (1988) *Biochemistry 27*, 8063−8068.
21. Raschke, T. M., and Marqusee, S. (1997) *Nat. Struct. Biol. 4*, 298−304.
22. Kuwajima, K., Yamaya, H., Miwa, S., Sugai, S., and Nagamura, T. (1987) *FEBS Lett. 221*, 115−118.
23. Baldwin, R. L. (1996) *Folding Des. 1*, R1−R8.
24. Waldburger, C. D., Jonsson, T., and Sauer, R. T. (1996) *Proc. Natl. Acad. Sci. U.S.A. 93*, 2629−2634.
25. Shortle, D., and Meeker, A. K. (1986) *Proteins 1*, 81−89.
26. Shortle, D., and Meeker, A. K. (1989) *Biochemistry 28*, 936−944.
27. Green, S. M., Meeker, A. K., and Shortle, D. (1992) *Biochemistry 31*, 5717−5728.

BI000466U